Current Noise Spectrum and Capacitance Due to the Membrane Motor of the Outer Hair Cell: Theory

K. H. Iwasa
Biophysics Section, LCB, National Institute on Deafness and Other Communication Disorders, National Institutes of Health, Bethesda, Maryland 20892-0922 USA

ABSTRACT The voltage-dependent motility of the outer hair cell is based on a membrane motor densely distributed in the lateral membrane. The gating charge of the membrane motor is manifested as a bell-shaped membrane potential dependence of the membrane capacitance. In this paper it is shown that movements of the gating charge should produce a high-pass current noise described by an inverse Lorentzian similar to the one shown by Kolb and Läuger for ion carriers. The frequency dependence of the voltage-dependent capacitance is also derived. These derivations are based on membrane motor models with two or three states. These two models lead to similar predictions on the capacitance and current noise. It is expected that the examination of the spectral properties of these quantities would be a useful means of determining the relaxation time for conformational transitions of the membrane motor.

INTRODUCTION

The outer hair cell (OHC) is one of the mechanoreceptor cells in the cochlea. This receptor cell also has a voltage-dependent motility (Brownell et al., 1985) that is unique among cells in that it is independent of ATP (Holley and Ashmore, 1988), the ubiquitous chemical energy source, and insensitive to Ca^{2+} (Iwasa et al., 1995), the most common second messenger. Thus this sensory cell can work as a mechanical actuator or reverse transducer. For this reason, the OHC has been considered the cellular basis of an active process in the cochlea that contributes to the exquisite sensitivity of the ear to low-intensity sounds and to minute differences in their tones (see de Boer, 1991, for a review).

The membrane capacitance of the outer hair cell has a bell-shaped dependence on the membrane potential, indicating the existence of numerous charges that move across the membrane (Ashmore, 1990; Santos-Sacchi, 1991; Iwasa, 1993). In addition, the membrane capacitance is also dependent on the membrane tension (Iwasa, 1993; Gale and Ashmore, 1994; Kakehata and Santos-Sacchi, 1995). These observations provide evidence that charge movements are directly coupled with mechanical changes and thus show that the motility of the OHC is driven by a membrane motor that directly utilizes electrical energy obtained at the plasma membrane (Iwasa, 1993, 1994; Iwasa and Adachi, 1997).

Conformational fluctuations of the motor produce current noise, because transitions between the states accompany charge transfers across the membrane. Thus it is expected that the current noise spectrum reflects transition rates between the states. It is shown in the present paper that movements of motor charges lead to a high-pass current noise, described as an inverse Lorentzian. A similar spectral characteristic has been obtained for current noise of ion carriers (Kolb and Läuger, 1978; Benz et al., 1989) and hydrophobic ions (Szabo, 1977; Kolb and Läuger, 1977). Movements of motor charges also contribute to the membrane capacitance, which is similar to the effect of hydrophobic ions (Szabo, 1977; Fernandez et al., 1983). The spectral shape of the capacitance is expressed by a Lorentzian (or a Debye function). These derivations are simplest if the motor has only two states. A motor with three states that differ in charge is also examined as the next simplest case of multistate motors. The frequency dependence of the current noise and the membrane capacitance are expected to provide estimates of transition rates of the motor, supplementing earlier reports (Dallos and Evans, 1995; Ashmore and Gale, 1997).

A TWO-STATE MODEL

Let us consider a motor protein in the membrane and assume that the motor has two conformational states, 0 and 1. These two states differ in electric and mechanical properties. During transitions between these states, a charge q is transferred across the membrane. These two states also occupy different cross-sectional areas in the membrane. The membrane motor is based on the coupling of charge transfers and changes in the cross-sectional area (Iwasa, 1993, 1994; Iwasa and Adachi, 1997). The probability P_1 that the motor is in state 1 follows a differential equation,

$$\frac{dP_1}{dt} = -k_- P_1 + k_+(1 - P_1), \qquad (1)$$

where k_+ is the transition rate from state 0 to state 1 and k_- is the rate from state 1 to state 0. The equilibrium condition

Received for publication 14 May 1997 and in final form 10 September 1997.

Address reprint requests to Dr. Kuni H. Iwasa, Biophysics Section, Laboratory of Cell Biology, National Institute on Deafness and Other Communication Disorders, National Institutes of Health, Bldg. 9, Rm. 1E120, 9 Center Dr., MSC 0922, Bethesda, MD 20892. Tel.: 301-496-3987; Fax: 301-480-0827; E-mail: kiwasa@helix.nih.gov.

0006-3495/97/12/2965/07 $2.00

satisfies

$$\frac{P_1}{1-P_1}=\frac{k_+}{k_-}=\exp\left[-\frac{\Delta F}{k_BT}\right] \tag{2}$$

where k_B is the Boltzmann constant, T is the temperature, and ΔF is the difference in the free energy F_0 and F_1 in the two states,

$$\Delta F=\Delta F_0+qV_m. \tag{3}$$

Here ΔF_0 is the sum of nonelectrical terms in the free energy difference, including mechanical ones; q is the difference in the charge in the two states; and V_m is the membrane potential. In the following, the power spectrum of current noise is derived through the complex admittance of this system.

Let the membrane potential V_m consist of two parts,

$$V_m=V_0+v_0\exp[i\omega t] \tag{4}$$

namely, a constant term V_0 and sinusoidal wave with an angular frequency ω and a small amplitude v_0. With Eq. 4, the ratio of the two rates is expressed by the transition rates $\bar{k}_+$ and $\bar{k}_-$ at the voltage V_0 by

$$\frac{k_+}{k_-}=\frac{\bar{k}_+}{\bar{k}_-}(1-u_0\exp[i\omega t]) \tag{5}$$

assuming that the quantity

$$u_0=\frac{qv_0}{k_BT} \tag{6}$$

is small. Putting the transition rates

$$k_-=\bar{k}_-\left(1+\frac{\bar{k}_+u_0}{\bar{k}_++\bar{k}_-}\exp[i\omega t]\right) \tag{7a}$$

$$k_+=\bar{k}_+\left(1-\frac{\bar{k}_-u_0}{\bar{k}_++\bar{k}_-}\exp[i\omega t]\right) \tag{7b}$$

which satisfy Eq. 5 and the condition $k_-=\bar{k}_-$ and $k_+=\bar{k}_+$ at $v_0=0$, enables us to write down the differential Eq. 1 in a simple form:

$$\frac{dP_1}{dt}=\bar{k}_+-\bar{P}_1k_-u_0\exp[i\omega t]-(\bar{k}_++\bar{k}_-)P_1 \tag{8}$$

with the steady-state value for P_1,

$$\bar{P}_1=\frac{\bar{k}_+}{\bar{k}_++\bar{k}_-}. \tag{9}$$

Equation 7 for the transition rates keeps the mean value of P_1 independent of the amplitude v_0, although it is not unique in satisfying Eq. 5. Equation 8 is simplified by introducing the difference p between P_1 and P_1,

$$p=p_0\exp[i\omega t]=P_1-\bar{P}_1$$

The complex amplitude p_0 of the quantity p at the angular frequency ω satisfies

$$p_0=-\frac{\bar{P}_1\bar{k}_-u_0}{i\omega+\bar{k}_++\bar{k}_-}. \tag{10}$$

ADMITTANCE FUNCTION

The membrane current due to the motor charge is proportional to the rate of transitions of the motor. If a cell has N motor units, the membrane current I of the cell is represented by

$$I(t)=-qN\frac{dP_1}{dt}. \tag{11}$$

With Eqs. 8 and 9, the current is then expressed in terms of p_0. Since this current was produced in response to small voltage changes $v(t)=v_0\exp[i\omega t]$, the complex admittance $Y(\omega)$ of the membrane is obtained:

$$Y(\omega)=\frac{I(t)}{v(t)}=\frac{q^2N\bar{k}_+\bar{k}_-}{(\bar{k}_++\bar{k}_-)k_BT}\cdot\frac{i\omega}{i\omega+\bar{k}_++\bar{k}_-}. \tag{12}$$

The power spectrum $S_I(\omega)$ of current noise is in general related to the admittance by the equation (Nyquist, 1928; Kubo, 1957)

$$S_{I,motor}(\omega)=4k_BT\,\mathrm{Re}[Y(\omega)].$$

Thus the power spectrum of the current noise due to the motor is

$$S_{I,motor}(\omega)=\frac{4q^2N\bar{k}_+\bar{k}_-}{\bar{k}_++\bar{k}_-}\cdot\frac{\omega^2}{\omega^2+(\bar{k}_++\bar{k}_-)^2}. \tag{13}$$

This power spectrum function is an inverse Lorentzian with a characteristic frequency, $\omega_2=\bar{k}_++\bar{k}_-$. Examples are shown in Fig. 1. The derivation of Eq. 13 is similar to the one used for ion carriers by Kolb and Läuger (1978).

The complex admittance of the membrane is also related to the membrane capacitance. If the admittance is purely capacitative, the admittance is

$$Y(\omega)=i\omega C.$$

Thus the membrane capacitance is obtained by

$$C_{motor}(\omega)=\mathrm{Im}\left[\frac{Y(\omega)}{\omega}\right]=\frac{q^2N\bar{k}_+\bar{k}_-}{k_BT}\cdot\frac{1}{\omega^2+(\bar{k}_++\bar{k}_-)^2} \tag{14}$$

which is Lorentzian. Examples are shown in Fig. 2. The relaxation time is characterized by the frequency, $\omega_2=\bar{k}_++\bar{k}_-$. Equation 14 shows that the motor capacitance is zero in the high-frequency limit. This is because the motor charge cannot respond to a field alternating at a frequency higher than the characteristic frequency ω_2 of the motor. At

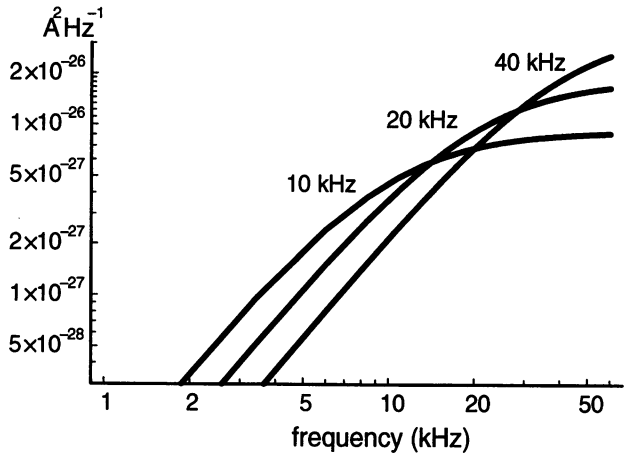

FIGURE 1 Power spectra of the current noise associated with the membrane motor with two states. The plot corresponds to Eq. 13 and the membrane potential that satisfies the condition $k_+ = k_-$, which maximizes the noise as well as the capacitance. The spectra shown correspond to three characteristic frequencies: 10 kHz, 20 kHz, and 40 kHz. Values for the parameters: $q = -0.9e$, $T = 300$ K, and $N = 7 \times 10^6$, which corresponds to the whole cell.

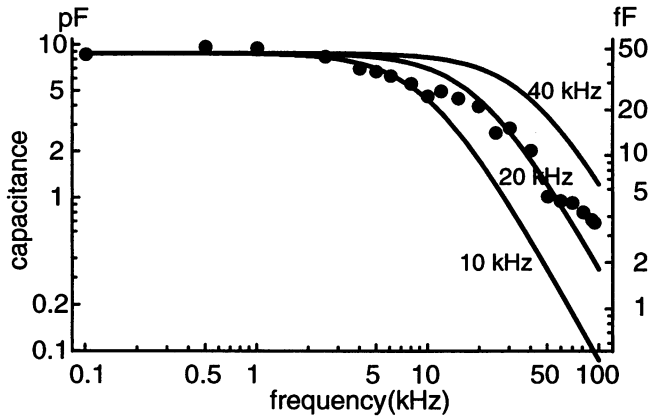

FIGURE 2 Frequency dependence of the membrane capacitance associated with the membrane motor with two states. The full lines correspond to Eq. 15, at the membrane potential that satisfies the condition $k_+ = k_-$, which maximizes the noise as well as the capacitance. The spectra with three characteristic frequencies are shown. They are 10 kHz, 20 kHz, and 40 kHz. Values for the parameters: $q = -0.9e$, $T = 300$ K, and $N = 7 \times 10^6$, which corresponds to the whole cell. The scale is shown on the left. Filled circles represent experimental data of Ashmore and Gale (1997) obtained from an on-cell patch, which has three relaxation frequencies: 9.2 kHz, 30 kHz, and 62 kHz. The scale of the experimental data is on the right.

the low-frequency limit, the capacitance is

$$C_{\text{motor}}(0) = \frac{q^2 N \bar{k}_+ \bar{k}_-}{k_B T} \cdot \frac{1}{(\bar{k}_+ + \bar{k}_-)^2} = \frac{q^2 N}{k_B T} P_1(1 - P_1) \qquad (15)$$

agreeing with the previous result (Iwasa, 1993, 1994), which was obtained by assuming that the transitions are infinitely fast.

Why does the noise spectrum have a high-pass characteristic? The source of the motor noise is the randomness in the flipping of the motor charges. For time intervals shorter than the relaxation time of the motor, these flips are uncorrelated because these motors cannot act quickly to cancel the free energy increases which these flips may have caused. For time intervals longer than the relaxation time of the motor, a motor tends to flip to lower the free energy of the system, which is elevated by a flip of another motor in the opposite direction. For this reason, for intervals longer than the relaxation time, current fluctuations are less than the level determined by random transitions. In the limit of extremely long time intervals, the current disappears because no DC current can be produced by these motor charges.

Thus the noise amplitude decreases when the frequency decreases beyond the characteristic frequency that corresponds to the relaxation time. The amplitude at the zero frequency limit is zero.

COMPARISON WITH A THREE-STATE MODEL

It is of importance to examine a model with more than two states to determine whether the two-state model described above gives larger current fluctuations than more complicated models. It would be easily expected that a multistate model gives rise to results similar to those of the two-state model if the kinetics of the multistate model has a single rate-limiting step. For this reason, the simplest and most interesting test would be the examination of a three-state model, where each transition between the states has equal importance. Specifically, the three-state model examined here has two transitions with identical transition rates, equal charge transfers, and equal area changes (see Eq. A1 in the Appendix).

How does such a three-state model compare with the two-state model described above in generating current fluctuations? It is not immediately obvious which model produces larger fluctuations. One of the important constraints for the models is to have the measured voltage dependence of the capacitance. To satisfy this condition, the three-state model needs to have a smaller unit charge transferred across the membrane at each transition, because having two similar transitions sharpens the voltage dependence of the capacitance. However, the three-state motor has more transitions per unit. In addition, the number of motor units in these two models may differ. Thus it is not obvious which model generates more current fluctuations. A detailed description of a three-state model given in the Appendix shows that there is no significant difference between these two models.

Let us start the comparison of the two models at a low frequency limit. This limit should be described as an equilibrium property. The current noise due to the motor diminishes at the limit of zero frequency and will be well below other noise sources. The contribution of the motor to the membrane capacitance at the limit of zero frequency is dependent on the membrane potential through the ratio of the transition rates (cf. Eqs. 15 and A13). Although the

two-state motor and the three-state motor do not lead to an identical function of the membrane potential, they are practically indistinguishable, because small differences at the two extremes of the membrane potential are hard to determine (Fig. 3). If these two forms are used to fit a given set of experimental data, they produce a somewhat different set of q and N. Thus experimental determination of these quantities is somewhat model dependent. The spectral characteristics of two models can be compared by using those different sets of values for q and N, which give indistinguishable voltage dependence of the capacitance in the zero frequency limit.

Another important factor in comparing the current noise and the capacitance due to different motor models is their relaxation time. Whereas the two-state motor has only a single relaxation frequency, the three-state motor has two (see Eq. A11). Let us first choose the membrane potential at which the membrane capacitance associated with the motor is maximized. This condition maximizes the current noise. If the same value $2\pi k$ is given for the transition rates in both directions, the characteristic frequency for the two-state model is $2k$, and those for the three-state model are k and $3k$ (see Eqs. 13 and A11). It is found numerically that the spectral shapes of both the capacitance and the current noise spectra are almost identical if the lower characteristic frequency for the three-state motor is equal to the characteristic frequency of the two-state motor (Figs. 4 and 5). Thus the distinction of whether the motor has two states or three states does not have a significant effect for these quantities.

DETECTION OF MOTOR NOISE IN THE CELL MEMBRANE

In addition to the motor, the plasma membrane has three other components of current noise, as described by numerous earlier studies (see DeFelice, 1981, for a review).

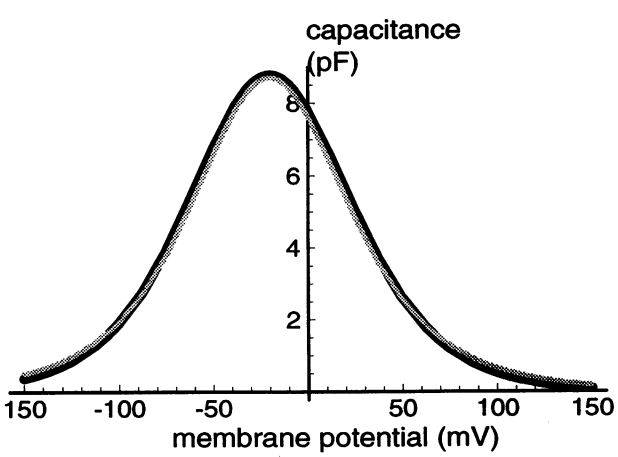

FIGURE 3 Voltage dependences of the membrane capacitance associated with the membrane motor in the zero-frequency limit. Comparison of two-state membrane motor (*dark line*) with three-state membrane motor (*gray line*). Values for the parameters: $q_2 = -0.9e$, $N_2 = 7 \times 10^6$; $N_3 = 0.68N_2$, $q_3 = 0.74q_2$.

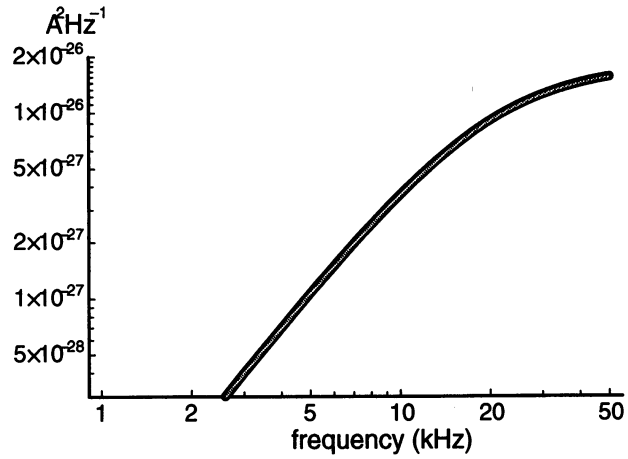

FIGURE 4 Comparison of the current noise spectrum associated with the two-state membrane motor and that associated with a three-state membrane motor. These plots are related to Eq. 13 (*dark line*) and Eq. A12 with A11 (*gray line*). The values for the transition rates are $k_+ = k_- = 6.28 \times 10^4$ for the two-state motor and $k_+ = k_- = 1.26 \times 10^5$ for the three-state motor. The characteristic frequency for the two-state motor is 2×10^4 Hz, and the characteristic frequencies for the three-state motor are 2×10^4 and 6×10^4 Hz. Other parameter values used are $q_2 = -0.9e$, $N_2 = 7 \times 10^6$; $N_3 = 0.68N_2$, $q_3 = 0.74\ q_2$, so that the voltage profiles of the capacitance are similar (see Fig. 3).

Among these, dominant sources under physiological conditions are channel noise and $1/f$ noise. Below 1 kHz, $1/f$ noise is usually not important. The noise due to channels is a sum of Lorentzians, which depend on their unit conductance, open probability, and transition rates. Although the relaxation times of most channels could be up to ~1 kHz,

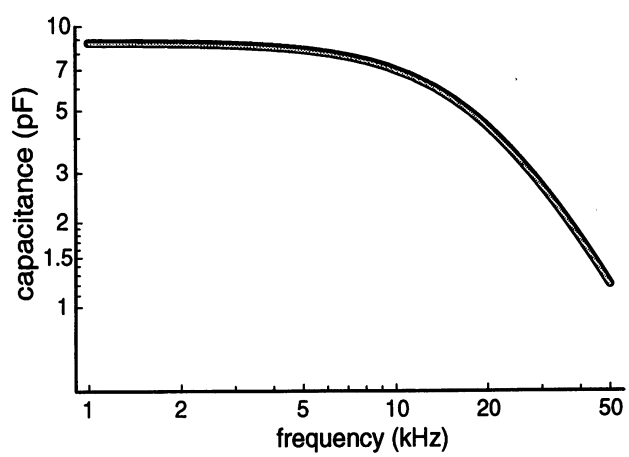

FIGURE 5 Comparison of the membrane capacitance associated with the two-state membrane motor and the one associated with a three-state membrane motor. These plots are related to Eq. 13 (*dark line*) and Eq. A12 with A11 (*gray line*). The values for the transition rates are $k_+ = k_- = 6.28 \times 10^4$ for the two-state motor and $k_+ = k_- = 1.26 \times 10^5$ for the three-state motor. The characteristic frequency for the two-state motor is 2×10^4 Hz, and the characteristic frequencies for the three-state motor are 2×10^4 and 6×10^4 Hz. Other parameter values used are $q_2 = -0.9e$, $N_2 = 7 \times 10^6$; $N_3 = 0.68N_2$, and $q_3 = 0.74q_2$, so that the voltage profiles of the capacitance are similar (see Fig. 3).

channel noise would still be overwhelming at higher frequencies because of its large amplitude. If adequate blocking media are used, the outer hair cell has a membrane resistance on the order of 1 GΩ (Kakehata and Santos-Sacchi, 1995). The expected noise above 1 kHz under this condition could then be given by the Nyquist formula (Nyquist, 1928),

$$S_{I,rest}(\omega) = 4k_BT/R_m$$

where R_m is the membrane resistance. This gives a noise floor of $\sim 1.7 \times 10^{-29}$ A^2s, which is orders of magnitude smaller than the expected levels of the motor noise (Fig. 1). Thus the motor noise could be observed above the Nyquist noise.

Another factor important for measuring the motor noise is frequency characteristics of the recording configuration. Whole-cell recording configuration has access resistance R_a of the pipette, which is between 3 MΩ and 5 MΩ, connected in series to the membrane resistance R_m, which should be at least ~1 GΩ, and the membrane capacitance C_m, ~20 pF. This circuit has a low-pass characteristic with a time constant R_aC_m from 60 μs to 100 μs, which corresponds to the frequency between 1.6 kHz and 2.7 kHz. This low-pass filtering characteristic is not compatible with a noise spectrum measurement that would require more than 10 kHz (Fig. 1).

For this reason, the whole-cell configuration is unsuitable for either noise spectrum or the frequency dependence of the membrane capacitance. Other variations of patch-clamp techniques, either on cell patch or detached patch configuration, do not have this difficulty. In these configurations, however, the seal of the pipette could dominate the resistance, reducing the signal-to-noise ratio. To improve the ratio, a giant patch configuration (Hilgemann, 1995) would be preferable to the conventional patch method. A giant patch has a larger membrane area within the pipette, but has a seal resistance similar to that of the conventional patches. This method thus reduces the relative importance of the seal and may have a good signal-to-noise ratio. If a membrane patch of ~100 μm^2 area is formed, the signal expected is between 1/10 and 1/20 of the whole cell. This condition allows observation of the motor noise if a good seal is formed. A preliminary result (Ehrenstein and Iwasa, 1997) indicates that this is indeed the case. The data obtained so far only allow the evaluation of a lower bound for the relaxation time, which is ~15 kHz. The relaxation time of 15 kHz is about the same as that in previous reports (Dallos and Evans, 1995; Ashmore and Gale, 1997).

EFFECT OF ELECTROMECHANICAL COUPLING

In the treatment of the membrane motor given above, conformational transitions of the motor were regarded as transfers of charges across the membrane. The effect of these transitions on the mechanical state of the system did not appear explicitly. Because conformational transitions of the motor are coupled with motions of the system, transitions between the motor states are subjected to mechanical constraints. For this reason, the relaxation time obtained from experiments may reflect the mechanical constraints imposed by experimental designs rather than the intrinsic property of the motor.

Consider, for example, a pulse protocol for determining the motor charge movements in a membrane patch (the experimental data in Fig. 2). Because a pulse larger than 10 mV in amplitude can elicit a membrane patch movement detectable by optical means (Ashmore and Gale, 1997), such movements of the membrane patch require movements of a water column in the patch pipette. Thus movements of water in the pipette and not transitions of an individual motor could be the factor that determines the rate of motor transitions in this configuration. For this reason, it is possible that the time course of the charge movement reflects the property of the water column in the patch pipette rather than the intrinsic relaxation time of the membrane patch or the motor. In this regard, the existence of multiple relaxation frequencies in the experimentally determined frequency dependence of the capacitance (Fig. 2) could be suggestive of multiple relaxation processes in the experimental configuration. One of the relaxation frequencies could be related to water movements and another to the intrinsic property of the motor.

If the effect of water in constraining the motor is significant, the membrane capacitance, which is usually determined with methods using an externally applied voltage waveform of considerable amplitude, could roll off at lower frequencies without the corresponding rise in the current noise, because water would suppress the movement of the motor in these conditions. For this reason, examining the noise spectrum would be critically important for determining the limiting factor of motor movements.

DETERMINATION OF DETAILED PROPERTIES OF THE MOTOR

The size of the gating charge is related to the voltage dependence of the capacitance. As elaborated above, however, this dependence still leaves some uncertainty in determining the unit charge that is transferred across the membrane during each transition of the membrane motor. If it is possible to know the number of states the motor can take, the unit charge transferred can be determined by the voltage dependence of the capacitance. The problem is that the voltage dependence of the capacitance does not provide sufficient information to unequivocally determine the number of states the motor can take. For example, a two-state model and a three-state model give rise to voltage dependences so close that they are practically indistinguishable. These two models, which produce indistinguishable results, give somewhat different values for the gating charge, however, as elaborated earlier.

An alternative method for determining the gating charge would be to examine the current-current variance plot for

nonstationary current (Conti and Stühmer, 1989; Heinemann and Conti, 1992). This method, however, requires that the sampling interval of data acquisition be shorter than the characteristic time constant of the motor. This requires that a bandwidth for data acquisition be wide enough to be able to cover the saturating range of the current noise spectrum. As discussed above, even with the bandwidth with which roll-off of the membrane capacitance is observed (Ashmore and Gale, 1997), the saturated value of the noise spectrum may not be observed. Thus with this bandwidth, the current-current variance plot may not be useful in determining the gating charge.

It is thus expected that analyses of the noise associated with the membrane motor provide information useful for clarifying the transition rates of the motor, mechanical constraints imposed on the motor, and the feasibility of methods for motor charge determination, even if they may not lead to unequivocal determination of the kinetic properties of the membrane motor.

APPENDIX: A THREE-STATE MODEL

To clarify the effect of multiple states with each transition involving charge transfer across the membrane, let us consider a system of N^* membrane motors with three conformational states, 0, 1, and 2. An individual motor undergoes the following transitions:

$$0 \underset{k_-}{\overset{k_+}{\rightleftharpoons}} 1 \underset{k_-}{\overset{k_+}{\rightleftharpoons}} 2 \tag{A1}$$

For simplicity, the transition rate to a state with a higher number is represented by k_+, and the one in the other direction by k_-. We assume that the same charge q^* is transferred across the membrane during the transition between states 0 and 1 and during the transition between state 1 and state 2. The transitions between the states are described by the differential equation,

$$\frac{\mathrm{d}}{\mathrm{d}t}\begin{pmatrix} P_0 \\ P_1 \\ P_2 \end{pmatrix} = \begin{pmatrix} -k_+ & k_- & 0 \\ k_+ & -k_+ - k_- & k_- \\ 0 & k_+ & -k_- \end{pmatrix}\begin{pmatrix} P_0 \\ P_1 \\ P_2 \end{pmatrix} \tag{A2}$$

where P_0, P_1, and P_2 are the probabilities that the motor is in states 0, 1, or 2, respectively. These probabilities satisfy $P_0 + P_1 + P_2 = 1$. The membrane current $I_3(t)$ of the three-state motor system is the time derivative of the charge Q_3,

$$Q_3(t) = N^* q^* (P_1 + 2 \cdot P_2). \tag{A3}$$

Here the subscript 3 indicates the three-state motor. As in Eq. 2, the ratio of the transition rates is described by

$$\frac{k_+}{k_-} = \exp\left[-\frac{\Delta F}{k_B T}\right]$$

where the free energy difference ΔF includes the electric term, expressed as in Eq. 3. The electric charge q must be substituted by q^*. Thus k_+ and k_- can be expressed as in Eq. 7,

$$\begin{aligned} k_+ &= \bar{k}_+ - ku \\ k_- &= \bar{k}_- + ku \end{aligned} \tag{A4}$$

where the quantities k and u are defined by

$$\begin{aligned} u &= u_0 \exp[i\omega t], \\ k &= \frac{\bar{k}_+ \bar{k}_-}{\bar{k}_+ + \bar{k}_-}. \end{aligned} \tag{A5}$$

The probabilities P_1 and P_2 that the motor is in state 1 or state 2, respectively, should consist of two parts,

$$\begin{aligned} P_1 &= \bar{P}_1 + p_1 \\ P_2 &= \bar{P}_2 + p_2 \end{aligned} \tag{A6}$$

namely, steady-state components, P_1 and P_2, and time-dependent parts, p_1 and p_2. The steady-state components satisfy

$$\bar{P}_1 = \frac{\bar{k}_+ \bar{k}_-}{\bar{k}_+^2 + \bar{k}_+ \bar{k}_- + \bar{k}_-^2}, \tag{A7}$$

$$\bar{P}_2 = \frac{\bar{k}_+^{\,2}}{\bar{k}_+^2 + \bar{k}_+ \bar{k}_- + \bar{k}_-^2}.$$

The time-dependent components satisfy the differential equations

$$\begin{aligned} \frac{\mathrm{d}p_1}{\mathrm{d}t} &= -(2\bar{k}_+ + \bar{k}_-)p_1 + (\bar{k}_- - \bar{k}_+)p_2 + (\bar{P}_1 + 2\bar{P}_2 - 1)ku \\ \frac{\mathrm{d}p_2}{\mathrm{d}t} &= \bar{k}_+ p_1 - \bar{k}_- p_2 - (\bar{P}_1 + \bar{P}_2)ku \end{aligned} \tag{A8}$$

if higher-order terms can be ignored. Because both p_1 and p_2 have the frequency ω, it is easy to see with Eqs. A3 and A8 that

$$Q_3(t) = \frac{i\omega k_2 + k_2^2 + 2\bar{k}_+ \bar{k}_-}{\omega^2 - 2i\omega k_2 - k_3} \cdot \frac{\bar{k}_+ \bar{k}_- u q^* N^*}{k_3} \tag{A9}$$

where k_2 and k_3 are defined by

$$\begin{aligned} k_2 &= \bar{k}_+ + \bar{k}_-, \\ k_3 &= \bar{k}_+^2 + \bar{k}_+ \bar{k}_- + \bar{k}_-^2. \end{aligned} \tag{A10}$$

The admittance of the membrane is obtained by current per voltage change, and here membrane current is obtained as the time derivative of Q_3. This leads to the admittance $Y_3(\omega)$ for the three-state motor,

$$Y_3(\omega) = \frac{\omega[\omega k_2 - i(k_2^2 + 2\bar{k}_+ \bar{k}_-)]}{\omega^2 - 2i\omega k_2 - k_3} \frac{\bar{k}_+ \bar{k}_- q^{*2} N^*}{k_3 k_B T}. \tag{A11}$$

The admittance has two characteristic frequencies; these are $k_+ + k_- \pm \sqrt{k_+ k_-}$. The power spectrum $S_{I,3}(\omega)$ of current and the membrane capacitance $C(\omega)$ are obtained from the admittance function,

$$\begin{aligned} S_{I,3}(\omega) &= 4k_B T \,\mathrm{Re}[Y_3(\omega)], \\ C_3(\omega) &= \mathrm{Im}[Y_3(\omega)/\omega]. \end{aligned} \tag{A12}$$

The frequency dependencies of these quantities are shown in Figs. 4 and 5. With Eqs. A11 and A12, the membrane capacitance $C_3(0)$ due to the three-state motor in the low-frequency limit has the form

$$C_3(0) = \frac{P(1-P)[1 + 2P(1-P)]}{[1 - P(1-P)]^2} \frac{q^{*2} N^*}{k_B T} \tag{A13}$$

where the voltage dependence of P is the same as that of P_1 in the main body of the text, which is expressed by Eq. 2.

Although the voltage dependence of Eq. A13 is not the same as that of Eq. 15, they are experimentally hard to distinguish, because the two constants q (or q^*) and N (or N^*) serve as adjustable parameters (Fig. 3). These two models give somewhat different values for the charge transferred across the membrane during each conformational transition of the motor and the number of the motor (Iwasa, 1996).

The author thanks Dr. Richard Chadwick, Dr. Gerald Ehrenstein, and two anonymous reviewers for comments.

REFERENCES

Ashmore, J. F. 1990. Forward and reverse transduction in the mammalian cochlea. *Neurosci. Res.* Suppl. 12:S39–S50.

Ashmore, J. F., and J. E. Gale. 1997. The intrinsic limit for active cochlear mechanics. *In* Diversity in Auditory Mechanics. E. R. Lewis, G. R. Long, R. F. Lyon, P. M. Narins, C. R. Steele, and E. Hecht-Poiner, editors. World Scientific, Singapore. 481–486.

Benz, R., H. A. Kolb, P. Läuger, and G. Stark. 1989. Ion carriers in planar bilayers: relaxation techniques and noise analysis. *Methods Enzymol.* 171:274–286.

Brownell, W. E., C. Bader, D. Bertrand, and Y. Ribaupierre. 1985. Evoked mechanical responses of isolated cochlear hair cells. *Science.* 227: 194–196.

Conti, F., and W. Stühmer. 1989. Quantal charge redistributions accompanying the structural transitions of sodium channels. *Eur. Biophys. J.* 17:53–59.

Dallos, P., and B. Evans. 1995. High-frequency motility of outer hair cells and the cochlear amplifier. *Science.* 267:2006–2009.

de Boer, E. 1991. Auditory physics. Physical principles in hearing theory III. *Phys. Rep.* 203:125–231.

DeFelice, L. J. 1981. Introduction to Membrane Noise. Plenum, New York.

Ehrenstein, D., and K. H. Iwasa. 1997. Current noise power spectrum of the membrane motor of the cochlear outer hair cell. *Biophys. J.* 72:A368.

Fernandez, J. M., R. E. Taylor, and F. Bezanilla. 1983. Induced capacitance in the squid giant axon. *J. Gen. Physiol.* 82:331–346.

Gale, J. E., and J. F. Ashmore. 1994. Charge displacement induced by rapid stretch in the basolateral membrane of the guinea-pig outer hair cell. *Proc. R. Soc. Lond.* B. 255:243–249.

Heinemann, S. H., and F. Conti. 1992. Nonstationary noise analysis and application to patch clamp recordings. *Methods Enzymol.* 207:131–148.

Hilgemann, D. W. 1995. The giant membrane patch. *In* Single Channel Recording. B. Sakmann and E. Neher, editors. Plenum, New York. 304–327.

Holley, M. C., and J. F. Ashmore. 1988. On the mechanism of a high-frequency force generator in outer hair cells isolated from the guinea pig cochlea. *Proc. R. Soc. Lond. B.* 232:413–429.

Housley, G. D., and J. F. Ashmore. 1992. Ionic currents of outer hair cells isolated from the guinea pig. *J. Physiol. (Lond.).* 448:73–98.

Iwasa, K. H. 1993. Effect of stress on the membrane capacitance of the auditory outer hair cell. *Biophys. J.* 65:492–498.

Iwasa, K. H. 1994. A membrane motor model for the fast motility of the outer hair cell. *J. Acoust. Soc. Am.* 96:2216–2224.

Iwasa, K. H. 1996. Membrane motors in the outer hair cell of the mammalian cochlea. *Comm. Theor. Biol.* 4:93–114.

Iwasa, K. H., and M. Adachi. 1997. Force generation in the outer hair cell of the cochlea. *Biophys. J.* 73:546–555.

Iwasa, K. H., M. Li, and M. Jia. 1995. Can membrane proteins drive a cell? *Biophys. J.* 68:214S.

Kakehata, S., and J. Santos-Sacchi. 1995. Membrane tension directly shifts voltage dependence of outer hair cell motility and associated gating charge. *Biophys. J.* 68:2190–2197.

Kolb, H. A., and P. Läuger. 1977. Electrical noise from lipid bilayer membranes in the presence of hydrophobic ions. *J. Membr. Biol.* 37: 321–345.

Kolb, H. A., and P. Läuger. 1978. Spectral analysis of current noise generated by carrier-mediated ion transport. *J. Membr. Biol.* 41: 167–187.

Kubo, R. 1957. Statistical-mechanical theory of irreversible processes. *J. Phys. Soc. Jpn.* 12:570–586.

Nyquist, H. 1928. Thermal agitation of electric charge in conductors. *Phys. Rev.* 32:110–113.

Santos-Sacchi, J. 1991. Reversible inhibition of voltage-dependent outer hair cell motility and capacitance. *J. Neurosci.* 11:3096–3110.

Szabo, G. 1977. Electrical characteristics of ion transport in lipid bilayer membranes. *Ann. N.Y. Acad. Sci.* 303:266–280.